

Chandra High-Resolution Camera Observations of the Luminous X-Ray Source in the Starburst Galaxy M82

P. Kaaret¹, A.H. Prestwich¹, A. Zezas¹, S.S. Murray¹, D.-W. Kim¹,
R.E. Kilgard¹, E.M. Schlegel¹ and M.J. Ward²

¹*Harvard-Smithsonian Center for Astrophysics, 60 Garden St., Cambridge, MA 02138, USA*

²*Department of Physics and Astronomy, University of Leicester, Leicester LE1 7RH, UK*

Accepted 2000. Received 2000 ; in original form 2000 August 8

ABSTRACT

We have analyzed early Chandra High Resolution Camera observations of the starburst galaxy M82, concentrating on the most luminous x-ray source. We find a position for the source of R.A. = $09^{\text{h}}55^{\text{m}}50^{\text{s}}.2$, decl. = $+69^{\circ}40'46''.6$ (J2000) with a 1σ radial error of $0.7''$ and report detection of an x-ray oscillation with a period in the range 573–613 s. The accurate x-ray position shows that the luminous source is not at the dynamical centre of M82 or coincident with any suggested radio AGN candidate. The detection of ~ 600 s oscillations excludes the possibility that the source is a supernova or remnant, suggests that the source is a compact object, and can be used to place an upper bound of $1.3 \times 10^6 M_{\odot}$ on the mass of the compact object. The x-ray luminosity suggests a compact object mass of at least $500 M_{\odot}$. Thus, the luminous source in M82 likely represents a new class of compact object with a mass intermediate between those of stellar mass black hole candidates and supermassive black holes found in the centres of galaxies.

Key words: black hole physics – galaxies: individual: M82 – galaxies: starburst – galaxies: stellar content – X-rays: galaxies

1 INTRODUCTION

One of the most enigmatic results to emerge from X-ray population studies of spiral and other luminous star forming galaxies is the discovery of unresolved X-ray sources which appear to have luminosities factors of 10 to 100's times the Eddington luminosity for a neutron star (e.g. Roberts & Warwick 2000; Zezas, Georgantopoulos, & Ward 1999; Wang, Immler, & Pietsch 1999; Colbert & Mushotzky 1999; Fabbiano, Schweizer, & Mackie 1997; Marston et al. 1995; for a review of early results see Fabbiano 1988). The origin of such sources is controversial. Some are located near the dynamical centre of the host galaxy, and hence may be low luminosity AGN. However, many are well outside the central regions of the galaxies, and hence an alternative explanation is required. Some of these highly luminous x-ray sources may be very luminous supernova remnants exploding into a dense interstellar medium (Fabian & Terlevich 1996). Finally, they may be accretion powered binary sources, in which case they are excellent black hole candidates with masses near or above $10 M_{\odot}$ (Makishima et al. 2000). Deciding between these various alternatives has been complicated by the limited spatial resolution of pre-Chandra X-ray missions.

One of the most extreme and controversial examples of a highly luminous x-ray source in a nearby galaxy is the bright X-ray source that dominates the central region of the nearby starburst galaxy M82. Previous Einstein, ROSAT, and ASCA observations have shown that this source is variable and is close to the centre of M82 (Watson, Stanger, & Griffiths 1984; Collura et al. 1994; Ptak & Griffiths 1999). It has been interpreted as a low luminosity AGN at the dynamical centre of M82 (Matsumoto & Tsuru 1999), a highly x-ray luminous supernova (Stevens, Strickland, & Wills 1999), and an accreting binary (Ptak & Griffiths 1999). In this paper we discuss early Chandra observations of M82 made using the High Resolution Camera (HRC; Murray et al. 1997). The central x-ray ‘source’ in M82 is resolved into several sources in the HRC observations. We present an analysis of the brightest Chandra source, and report detection of an x-ray oscillation with a period of 600 s from an observation when the source was particularly bright. Our results suggest that this source is a black hole with a mass intermediate between stellar-mass Galactic x-ray binaries and supermassive black holes. We describe the observations in § 2, the source position and flux in § 3, our timing analysis in § 4, and conclude in § 5.

2 OBSERVATIONS

M82 was observed with the Chandra X-Ray Observatory (CXO; Weisskopf 1988) using the High Resolution Camera (HRC; Murray et al. 1997) and the High-Resolution Mirror Assembly (HRMA; van Speybroeck et al. 1997) on 1999 Oct 28 04:24 UT to 14:48 UT for an exposure of 36 ks and on 2000 Jan 20 14:51 UT to 20:25 UT for an exposure of 18 ks. The HRC is a microchannel plate imager having very good spatial and time resolution, but essentially no energy resolution. Each photon detected by the HRC is time and position tagged, making possible timing studies of individual sources in crowded fields. The HRC contains a wiring error, discovered after launch (Seward 2000), which induces a 3–4 ms error in the event time tags for this observation. As we restrict ourselves to frequencies below 0.1 Hz, this error has no effect on the analysis presented below. The HRC position tags have a precision of $0.132''$, referred to as ‘one pixel’. This resolution oversamples the Chandra point spread function (PSF) which has a half-power diameter of $0.76''$ (Jerius et al. 2000). We used a 15.6 pixel radius to extract source light curves.

We applied aspect to X-ray events from the HRC and filtered the data using event screening techniques (Murray et al. 2000) to eliminate ‘ghost’ events produced by the HRC electronics. An image for each observation was generated from the filtered event lists, see Fig. 1. We used the standard Chandra software routine `wavdetect` to search for and determine the position of point sources (CIAO V1.1 Software Tools Manual). We found several sources in each observation including both transients and persistent sources. Here, we concentrate on the brightest source found. The other sources, including spectroscopy from observations with the Chandra Advanced CCD Imaging Spectrometer (ACIS; Bautz et al. 1998), will be described in a forth-coming paper (Ward et al. 2000).

3 POSITION AND FLUX

The brightest source in both observations is at a location of R.A. = $09^{\text{h}}55^{\text{m}}50^{\text{s}}.2$, decl. = $+69^{\circ}40'46''.6$ (J2000). Following the convention of naming sources in M82 via their offset from R.A. = $09^{\text{h}}51^{\text{m}}00^{\text{s}}$, decl. = $+69^{\circ}54'00''$ (B1950), we refer to this source as X41.5+60.4 in the remainder of the paper. For wider use, we also denote the source as CXOU J095550.2+694046. The position uncertainty is dominated by the accuracy of the aspect reconstruction which we take to have a 1σ radial error of $0.7''$ (Aldcroft et al. 2000).

The source lies $9''$ from the kinematic centre of M82 (Weliachew, Fomalont, & Greisen 1984), $12''$ from the $2.2\mu\text{m}$ peak (Rieke et al. 1980), $3.9''$ from the very luminous supernova remnant 41.95+57.5 (Kronberg & Wilkinson 1975; Wills et al. 1997), and $13''$ from the suggested AGN candidate 44.01+59.6 (Wills et al. 1997; Seaquist, Frayer, & Frail 1997; Wills et al. 1999). The 408 MHz radio flux at the position of X41.5+60.4 is below 2 mJy (Wills et al. 1997). The radio source 41.31+59.6, which is likely a compact supernova remnant (Muxlow et al. 1994; Allen & Kronberg 1998), lies near the edge of the error circle. The highly variable radio source 41.5+59.7 (Kronberg & Sramek 1985) lies

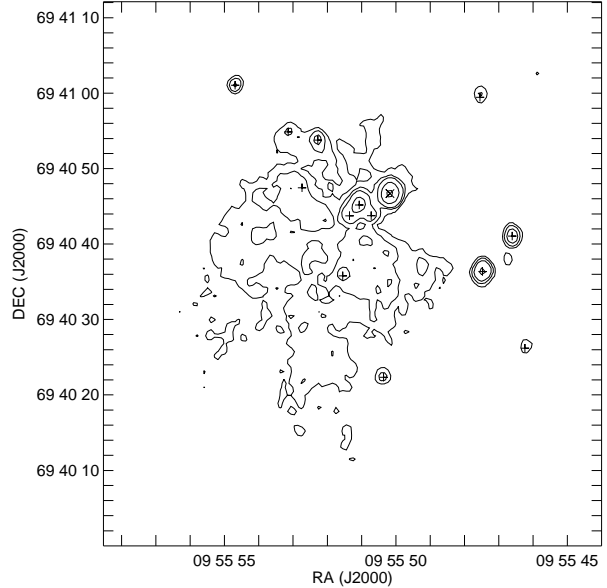


Figure 1. The central region of M82 from the October 1999 observation. The contours were calculated using a counts map with $0.53''$ pixels smoothed with a Gaussian with $\text{FWHM} = 1.06''$. The contours indicate 2.5, 5, 10, 40, and 160 counts per pixel in the smoothed map. The position of X41.5+60.4 is marked with an ‘X’. Crosses indicate positions of other sources.

within the error circle. This radio source was bright in one observation in 1981 but not detected one year later or subsequently, and has been interpreted as due to a supernova (Kronberg et al. 2000). However, as only one detection is available and unique identification is not possible based on the radio spectral index alone; the source may belong to a different class of radio transient (Muxlow et al. 1994).

X41.5+60.4 is highly variable. In the first observation, the HRC count rate from the source is 0.07 c/s , while in the second it is 0.52 c/s – a factor of 7 brighter. In the first observation, X41.5+60.4 accounts for roughly 40% of the counts within $6''$, i.e. comparable to the resolution of the ROSAT HRI, of the source position and only 8% of the counts within $4''$, i.e. comparable to the resolution of the ASCA SIS. In the second observation, X41.5+60.4 accounts for more than 90% of the counts within $6''$ and 40% within $4''$.

Using various spectral models consistent with the spectrum of this source extracted from a Chandra ACIS observation of M82 (Ward et al. 2000), we estimate that 1 c/s in the HRC corresponds to an observed flux of $0.9 - 1.4 \times 10^{-10}\text{ erg cm}^{-2}\text{ s}^{-1}$ in the 0.2–10 keV band. The range in the conversion factor is due to uncertainty in the ACIS spectral fits. The source flux in the ACIS observation corresponds to an HRC rate of 0.03 c/s , so the true conversion factors may differ from these values if the source spectrum varies with flux. The flux in the second observation is comparable to the highest fluxes observed from the central source in M82 with ASCA (Ptak & Griffiths 1999). Taking a distance to M82 of 3.63 Mpc (Freedman et al. 1994), the inferred isotropic source luminosity from the absorbed flux in the two observations would then be $1.0 - 1.5 \times 10^{40}\text{ erg s}^{-1}$ in the 0.2–10 keV band for the first observation and $7 - 11 \times 10^{40}\text{ erg s}^{-1}$ for

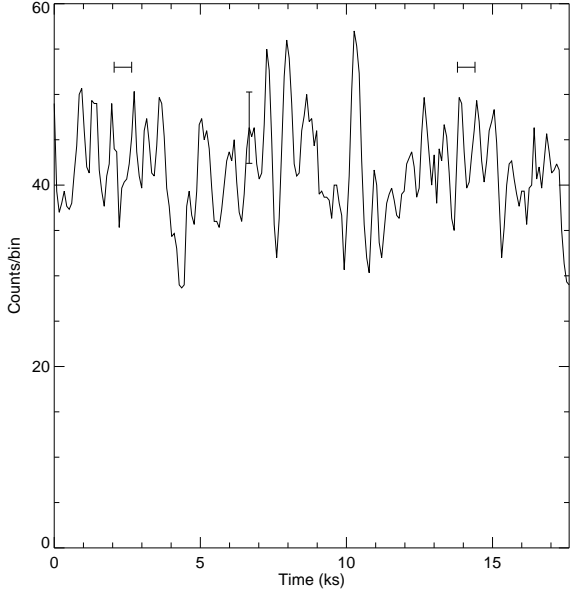


Figure 2. Light curve for the luminous source in M82 from the Chandra observation in January 2000. The time bin size is 85 s and the data were smoothed with a 3-element moving boxcar average for presentation purposes. A typical statistical error bar after application of the smoothing is shown. Two 600 s intervals are indicated by horizontal bars.

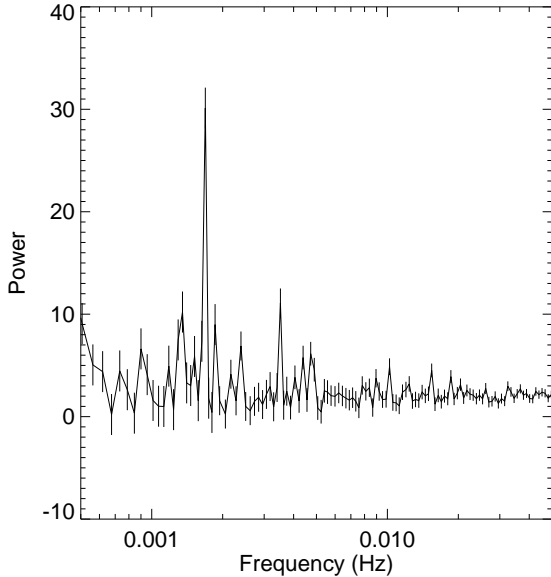


Figure 3. Power spectrum for the luminous source in M82. The power is Leahy normalized.

the second. Correcting for absorption would increase these luminosities; conversely, the true luminosity may be lower if the x-rays are beamed. These luminosities are near or above the highest values found for non-nuclear sources in a ROSAT sample of nearby galaxies (Roberts & Warwick 2000).

4 TIMING

For each observation, we extracted a light curve for X41.5+60.4 and then performed a Fourier transform to search for any possible periodicity. A light curve for the January 2000 observation is shown in Fig. 2 and a power spectrum in Fig. 3. There is a peak apparent near 1.69 mHz. The duration of the observation is 17769 s, leading to a frequency bin spacing of 0.056 mHz. The peak is not resolved in the power spectrum, and we place a lower bound on the coherence of $Q = \nu/\Delta\nu > 30$. The rms amplitude of the oscillation is 6%. The power spectrum for the October 1999 observation shows no significant peaks over the same frequency range.

The Chandra spacecraft is subjected to dither, a regular oscillation in pointing of the spacecraft, to spread the photons incident on the detector in order to prevent degradation of the performance of the HRC due to excessive charge build-up with a localized region of the detector and also (for both the HRC and ACIS) to average the detector response for an individual source over a large number of pixels (Chandra Observatory Proposer's Guide). Dither is a potential source of spurious timing signals and the dither frequencies for this observation are comparable to the frequency reported above, so we expended significant effort in the study of possible timing signals induced by the dither.

The Chandra dither consists of two distinct oscillation frequencies, one producing a modulation in the detector X coordinate and the other in the detector Y coordinate. Use of unequal frequencies in the two axes produces a Lissajous pattern of the source flux on the detector face. The dither periods are commandable. For the January 2000 observation the periods were 1086.96 s for X and 768.574 s for Y . We verified that these were the actual periods during the observation by examining the position of the luminous source in detector coordinates. There is a clear sinusoidal variation in the source position in detector coordinates with a period of 1087 ± 2 s for X and 769 ± 2 s for Y .

The two dither frequencies are distinct from the frequency reported above. However, in addition to the fundamental frequencies, the dither may also produce signals at sums, differences, and harmonics of the fundamentals. The dither-derived frequency closest to the frequency quoted above is twice the X dither frequency at 1.84 mHz. This frequency differs from the signal frequency by 3 frequency bins of the Fourier transform and, thus, is clearly resolved from the observed signal. To search for other potential instrumental effects, we simulated observations of a source with constant flux giving twice the count rate found from X41.5+60.4 in the January 2000 data using MARX (Wise et al. 2000) and the aspect data for the January observation. We found no significant peaks in power spectra for the frequency range 0.0005–0.05 Hz in the simulated data.

To further study the effects of dither on timing analysis of Chandra data, we varied the source extraction radius. A systematic error in the calculation of the dither position correction could lead to a situation where the motion of the source across the detector is incorrectly tracked by the dither correction. Thus, the location of the incident flux could vary relative to the location of the source extraction region in a manner correlated with the dither. Use of large extraction regions in which the PSF and therefore the source flux at

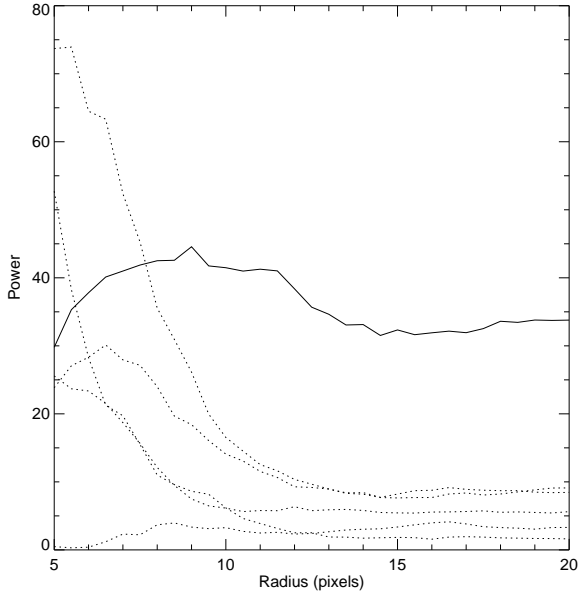


Figure 4. Power versus extraction radius for at the signal frequency of 1.69 mHz (solid line) and at five frequencies associated with dither (dotted lines) which are, in order of decreasing power at $r = 5.5$, ν_x , $\nu_y - \nu_x$, $\nu_y + \nu_x$, ν_y , and $2\nu_x$, where $\nu_x = 0.920$ mHz and $\nu_y = 1.301$ mHz are the X and Y dither frequencies, respectively. The power is Leahy normalized.

the boundary of the region is only a small fraction of the total flux minimizes such effects. Conversely, use of small extraction regions should magnify such effects. In Fig. 4, we plot the power at several frequencies associated with the dither and also the power at the frequency quoted above for circular source extraction regions with radii of 5–20 pixels. The powers at the frequencies associated with dither are low at large radii, become significant only at radii less than 10 pixels, and tend to increase sharply at small radii. In contrast, the power of the putative signal is high at large radii, is a maximum at moderate radii (where the signal to noise for the source is best), and decreases at small radii (where source photons are lost). The behavior of the putative signal is qualitatively different from the behavior of the signals associated with dither.

To check for effects related to the overall detector response, we generated a power spectrum for a region including diffuse emission and some point sources with a total count rate from the region larger than 0.6 c/s. We used a large region in order to have a high count rate and thus sensitivity similar to that in the power spectrum of X41.5+60.4. The power spectrum of the diffuse emission and other sources shows no significant peaks. This gives additional reassurance that the signal from X41.5+60.4 is not spurious.

As the oscillation may be coherent, we performed a periodicity search using the Z^2 or Rayleigh statistic (Buccheri, Ozel, & Sacco 1987) in a frequency range near the peak detected in the power spectrum. A peak value of 39.9 in the Z^2 statistic occurs at a frequency of 1.67 mHz. Folding the data at this frequency produces a roughly sinusoidal profile with a pulsed rate of 0.054 ± 0.009 c/s, equivalent to a pulsed fraction of 10% or an rms amplitude of 6%. A pulsation search of

the October 1999 data over the same frequency range leads to an upper bound on the pulsed rate of 0.015 c/s (95% confidence).

5 DISCUSSION

The luminosity of X41.5+60.4 in the January 2000 observation, given the assumptions concerning the spectral shape and isotropic emission noted above, corresponds to the Eddington luminosity for a 500 – 900 M_\odot object. The strong variability between observations argues against this luminosity being due to an aggregate of sources. The detection of a 600 s oscillation limits the physical size of the emitting region to 600 lt s = 1.2 AU and argues against origin in a supernova or supernova remnant. We considered the possibility that the oscillations are due to a transient x-ray pulsar in M82; however, even the modulated flux alone is substantially super-Eddington for an accreting neutron star and we exclude this possibility on that basis. Soft gamma repeaters (SGRs) produce sufficient flux and periodic signals. However, the longest, bright, so-called “giant”, outbursts from SGRs last only ~ 300 s over which they show substantial decay (Hurley et al. 1999). The fact that X41.5+60.4 shows no evidence of decay over 15 ks, see Fig. 2, argues against it being a SGR. Origin of the high luminosity and oscillations in a massive compact object appears plausible.

Quasiperiodic oscillations (QPOs) have been detected from stellar mass black hole candidates (BHCs), with frequencies in the 10 mHz – 300 Hz range, and reported from active galactic nuclei (AGN) with much lower frequencies: 1.7×10^{-5} Hz for IRAS 18325-5926 (Iwasawa et al. 1998) and 1.3×10^{-5} Hz for RX J0437.4-4711 (Halpern & Marshall 1996). The frequency reported here lies between these ranges and, since QPO frequency is generally thought to scale inversely with compact object mass, may suggest the presence of a compact object with a mass intermediate between the stellar mass BHCs and supermassive compact objects in AGN.

Assuming that the observed frequency cannot exceed the maximum allowed Keplerian orbital frequency around a Schwarzschild black hole, i.e. the orbital frequency at the marginally stable orbit at $r_{\text{ms}} = 6GM/c^2$, we can place an upper bound on the compact object mass of $M = M_\odot(\nu/2198\text{Hz})^{-1} = 1.3 \times 10^6 M_\odot$. Beyond this upper limit, deriving a firm mass estimate becomes somewhat problematic due to the wide range of frequencies observed from stellar mass BHCs. For example, GRO J1655-40 is a well studied stellar mass BHC for which there is an accurate dynamical mass determination of $7 M_\odot$ (Orosz & Bailyn 1997) and which shows QPOs at 300, 9, and 0.1 Hz and a variable frequency QPO in the range 14–28 Hz (Remillard et al. 1999). Comparison of the 1.67 mHz oscillation in X41.5+60.4 with these QPOs and scaling mass with the inverse of frequency (as is true for the maximum Keplerian orbital frequency) would lead to mass estimates of $1.3 \times 10^6 M_\odot$, $4 \times 10^4 M_\odot$, $400 M_\odot$, and $6 - 12 \times 10^4 M_\odot$, respectively.

If we assume that the accretion disk physics and QPO phenomenology of massive compact objects are similar to those of stellar mass BHCs, then some progress can be made. The QPO at 300 Hz from GRO J1655-40, corresponding to the maximum allowed orbital frequency, is observed only

when the luminosity exceeds $L_X \sim 0.2L_{\text{Edd}}$ (Remillard et al. 1999). If the 1.67 mHz oscillation in X41.5+60.4 corresponds to this QPO, then the corresponding luminosity would be $L_X \sim 0.2L_{\text{Edd}} = 3 \times 10^{43} \text{ erg s}^{-1}$, two orders of magnitude higher than the observed value. A further argument against identifying the oscillation from X41.5+60.4 with the maximum allowed orbital frequency is that the 300 Hz QPO has a low rms amplitude, less than 1%, in strong contrast to the rms amplitude of 6% seen in X41.5+60.4.

The strongest, narrow QPOs from Galactic BHCs tend to have frequencies in the range 0.1–20 Hz (e.g. Takizawa et al. 1997; Tomsick & Kaaret 2000) and somewhat lower for more massive BHCs (Morgan, Remillard, & Greiner 1997). These QPOs are often detected with rms amplitudes up to 15% and coherences up to $Q \sim 50$, similar to the properties of the oscillation from X41.5+60.4. Comparison of the 1.67 mHz oscillation in X41.5+60.4 with these QPOs leads to mass estimates in the range $400 - 8 \times 10^4 M_{\odot}$. These QPOs are seen in high ($L_X \sim L_{\text{Edd}}$) as well as low ($L_X \sim 0.02L_{\text{Edd}}$) luminosity states. Oscillation frequency is unlikely to depend on beaming angle, so these mass estimates are unaffected by beaming of the x-rays. The low oscillation frequency seen from X41.5+60.4 suggests that the high flux observed is not due to strongly beamed radiation from a stellar mass BHC.

In conclusion, detection of a 1.67 mHz oscillation from X41.5+60.4, the most luminous x-ray source in M82, rules out the possibility that it could arise from a supernova and places an upper bound on the potential compact object mass of $1.3 \times 10^6 M_{\odot}$. The accurate x-ray position determination, made possible by the high angular resolution of Chandra, excludes identification with suggested radio AGN candidates (Wills et al. 1997). The low radio flux at the x-ray position and the displacement of the source from the dynamical centre of M82 argue against X41.5+60.4 being a supermassive black hole similar to that seen at the centre of the Milky Way. The flux from the source places a lower bound on the compact object mass of $500 M_{\odot}$ if the emission is isotropic. The most plausible explanation for the object is that it is an accreting black hole with a mass of $500 - 10^5 M_{\odot}$. In this case, it represents a new class of compact object with a mass intermediate between those of stellar mass black hole candidates and supermassive black holes found in the centres of galaxies. While there is a broad understanding of the formation of super-massive black holes in galactic centers and of solar mass black holes, the formation and subsequent evolution of black holes with masses greater than $100 M_{\odot}$ outside of the nuclear region presents a challenge for the theory of the formation of compact objects (Taniguchi et al. 2000).

ACKNOWLEDGMENTS

We thank Tom Aldcroft for information concerning the dither and aspect solution. We gratefully acknowledge the efforts of the Chandra team and support from NASA Chandra contract NAS8-39073. PK acknowledges partial support from NASA grant NAG5-7405.

REFERENCES

Aldcroft T.L. et al. 2000, Proc. SPIE, to appear

- Allen M.L., Kronberg P.P. 1998, ApJ, 502, 218
 Bautz M.W. et al. 1998, Proc. SPIE, 3444, 210
 Buccheri R., Ozel M.E., Sacco B. 1987, A&A, 175, 353
 Chandra Observatory Proposer's Guide available at <http://asc.harvard.edu/udocs/docs/docs.html>
 Colbert E.J.M., Mushotzky R.F. 1999, ApJ, 519, 89
 Collura A., Reale F., Schulman E., Bregman J.N. 1994, ApJ, 420, L63
 Fabbiano G. 1989, ARA&A, 27, 87
 Fabbiano G., Schweizer F., Mackie G. 1997, ApJ, 478, 542
 Fabian A.C., Terlevich R. 1996, MNRAS, 280, L5
 Freedman W. et al. 1994, ApJ, 427, 628
 Jerius D. et al. 2000, Proc. SPIE, to appear
 Halpern J.P., Marshall H.L. 1996, ApJ, 464, 760
 Hurley K. et al. 1999, Nature, 397, 41
 Iwasawa K. et al. 1998, MNRAS, 295, L20
 Kronberg P.P., Wilkinson P.N. 1975, ApJ, 200, 430
 Kronberg P.P., Sramek R.A. 1985, Science, 227, 28
 Kronberg P.P., Sramek R.A., Birk G.T., Dufton Q.W., Clarke T.E., Allen M.L. 2000, ApJ, 535, 706
 Makishima K. et al. 2000, astro-ph/0001009
 Marston A.P., Elmegreen D., Elmegreen B., Forman W., Jones C., Flanagan K. 1995, ApJ, 438, 663
 Matsumoto H., Tsuru T.G. 1999, PASJ, 51, 321
 Morgan E.H., Remillard R.A., Greiner J. 1997, ApJ, 482, 993
 Murray S.S. et al. 1997, Proc. SPIE, 3114, 11
 Murray S.S. et al. 2000, Proc. SPIE, to appear
 Muxlow T.W.B., Pedlar A., Wilkinson P.N., Axon D.J., Sanders E.M., de Bruyn A.G. 1994, MNRAS, 266, 455
 Orosz J.A., Bailyn C.D. 1997, ApJ, 477, 876
 Ptak A., Griffiths R. 1999, ApJ, 517, L85
 Remillard R.A. et al. 1999, ApJ, 522, 397
 Rieke G.H., Lebofsky M.J., Thompson R.I., Low F.J., Tokunaga A.T. 1980, ApJ, 238, 24
 Roberts T.P., Warwick R.S. 2000, MNRAS, 315, 98
 Seaquist E.R., Frayer D.T., Frail D.A. 1997, ApJ, 487, L131
 Stevens I.R., Strickland D.K., & Wills K.A. 1999, MNRAS, 308, L23
 Takizawa M. et al. 1997, ApJ, 489, 272
 Taniguchi Y., Shioya Y., Tsuru T.G., Ikeuchi S. 2000, PASJ, 52, 533
 Tomsick J.A., Kaaret P. 2000, ApJ, 537, 448
 van Speybroeck L.P. et al. 1997, Proc. SPIE, 3113, 89
 Wang Q.D., Immler S., Pietsch W. 1999, ApJ, 523, 121
 Ward M.J. et al. 2000, in preparation
 Watson M.G., Stanger V., & Griffiths R.E. 1984, ApJ, 286, 144
 Weisskopf M.C. 1988, Space Science Reviews, 47, 47
 Weliachew L., Fomalont E.B., Greisen E.W. 1984, A&A, 137, 335
 Wills K.A., Pedlar A., Muxlow T.W.B., Wilkinson P.N. 1997, MNRAS, 291, 517
 Wills K.A., Pedlar A., Muxlow T.W.B., Stevens I.R. 1999, MNRAS, 305, 680
 Wise M.W., Davis J.E., Huenemoerder D.P., Houck J.C., Dewey D. 2000, "MARX 3.0 Technical Manual" available at <http://space.mit.edu/ASC/MARX>
 Zezas A.L., Georgantopoulos I., Ward M.J. 1999, MNRAS, 308, 302